# Methanol Adsorption in Isomorphously Substituted AlPO-34 Clusters and Periodic Density Functional Theory Calculations

**Lihua Kang,[†] Tao Zhang,[‡] Zhongmin Liu,[‡] and Ke-Li Han*,[†]**

*State Key Laboratory of Molecular Reaction Dynamics, Dalian Institute of Chemical Physics, Chinese Academy of Sciences, Dalian, 116023, People's Republic of China, and State Key Laboratory of Catalysis, Dalian Institute of Chemical Physics, Chinese Academy of Sciences, Dalian, 116023, People's Republic of China*

*Received: October 3, 2007; In Final Form: January 18, 2008*

Methanol adsorption in isomorphously substituted MAPO-34 (M = Mn, Zn, Mg, Si, Ti, or Zr) zeolite clusters was investigated, and periodic density functional theory (DFT) calculations were carried out. All structures are optimized and charactered at B3LYP/LANL2DZ-6-31G** (the LANL2DZ basis set for Mn, Zn, Mg, Ti, and Zr atoms and 6-31G** basis set sequentially for Si, Al, O, C, and H atoms) and generalized gradient approximation and Perder−Burke−Ernzerhof theoretical levels. Both methods demonstrate that the type of metal dopant used plays an active role in methanol protonation. In Mn, Zn, and Mg-AlPO-34, the stable form of methanol is protonated. However, in Si, Ti, and Zr-AlPO-34, methanol is unprotonated and is simply physisorbed. In the protonated mode, the methoxonium cation forms two very strong hydrogen bonds (1.019−1.073 Å) with the negatively charged zeolite. On the other hand, in the physisorbed mode, methanol interacts with the zeolite framework to form an eight-member ring through two hydrogen bonds, one that is short and rather strong (1.392−1.676 Å) and one that is much weaker (1.941−3.036 Å).

## 1. Introduction

The hydrogen form of zeolites is applied in many catalytic reactions such as the conversion of methanol to gasoline (MTG) process.[1] This is an important process that has attracted considerable attention from both industrial and academic researchers.[2−5] In the past decades, attention has been focused on H-ZSM-5.[6,7] Recently, metal-substituted aluminophosphates (MAPOs) have attracted considerable interest.[8−14] Although a significant number of studies have investigated the properties of isomorphously substituted zeolites,[15−20] our understanding of how heteroatoms modify the structure and electronic properties of acid sites, and thus, affect their adsorption and catalytic behaviors, is far from complete.[16,21,22] To the best of our knowledge, there are no reports in the literature of comparative studies of methanol adsorption in isomorphously substituted MAPO-34 (M = Mn, Zn, Mg, Si, Ti, or Zr) zeolite, which is an important catalyst for methanol-related reactions.

Many experimental and theoretical[23−34] studies have demonstrated that the first stage in the MTG reaction is the adsorption of methanol on the Bronsted acid sites of the zeolites network,[30] where the formation of a hydrogen-bonded or protonated methanol species is possible. However, the nature of the species formed on initial methanol adsorption is unclear from experiments, since infrared spectroscopy (IR)[35−37] and nuclear magnetic resonance (NMR)[38,39] techniques cannot distinguish unambiguously between physisorbed methanol, $CH_3$-OH-HOZ, and chemisorbed methanol, $CH_3OH_2^+$-$^-$OZ, where HOZ represents a zeolite Bronsted site and $^-$OZ represents a deprotonated acid site. In the last decades, theoretical studies[29−31,40,41] have started to shed light on the initial stages of the MTG process. Studies using clusters containing of the order of 10 tetrahedral atoms to model adsorption of a single methanol molecule at an acid site revealed that methanol was only physisorbed.[40,41] Recently, the adsorption of methanol in 8T (tetrahedral) rings was theoretically studied using DFT methods.[31,32] The results revealed that the hydrogen-bonding species are energetically favored with respect to the protonated system. However, a cluster has the major disadvantage of that it ignores all electrostatic interactions and the long-range influence of the zeolite lattice.[42,43] On the other hand, the use of a relatively large cluster can partly allow for consideration of the zeolite lattice.[44,45] Quantum-chemical periodic structure

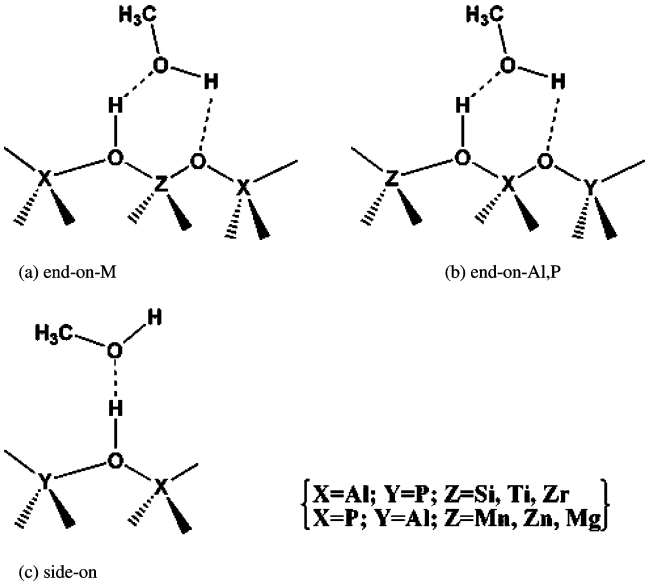


**Figure 1.** Schematic representation of the three adsorption modes: (a) end-on (bridging across metal), (b) end-on (bridging across Al or P), (c) side-on.

* To whom correspondence should be addressed. E-mail: klhan@dicp.ac.cn.

[†] State Key Laboratory of Molecular Reaction Dynamics, Dalian Institute of Chemical Physics, Chinese Academy of Sciences.

[‡] State Key Laboratory of Catalysis, Dalian Institute of Chemical Physics, Chinese Academy of Sciences.

10.1021/jp709669p CCC: $40.75 © 2008 American Chemical Society
Published on Web 03/18/2008

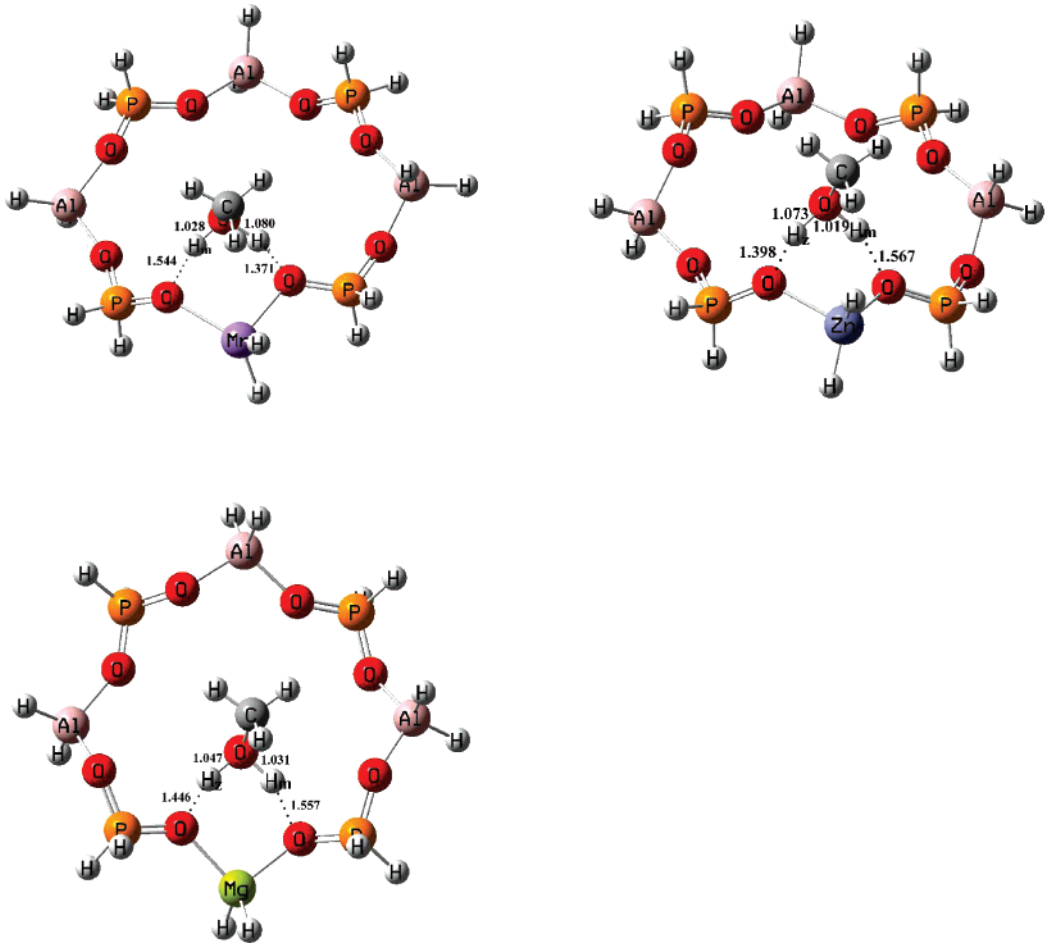


**Figure 2.** Equilibrium geometry found for $CH_3OH$ adsorbed on Mn-, Zn-, and Mg-AlPO-34 with the cluster models. Selected bond distances are given in angstroms.

codes are interesting, since it has recently become possible to localize approximate transition structures.[46] The role of the zeolite structure in the activation of methanol has been studied using a periodic approach, but the conclusions are somewhat contradictory. By comparison of the adsorption energy and geometry of methanol on different zeolites, Stich et al.[29] have concluded that protonation of a single methanol molecule may occur depending on the zeolite framework, whereas Haase et al.[30] have concluded that the zeolite framework does not have a decisive influence on either the adsorption energy or the geometry.[32] Thus, the goal of the present study was to resolve these issues and in particular to explore the factors identified as important in previous studies. We consider three factors: (1) Most notably, the cluster approach ignores long-range electrostatic potential, which may have a considerable effect given the partially ionic nature of zeolites. To compare the cluster results, we adopted another approach: use of periodic boundary conditions to simulate the full zeolite structure. (2) The acid strength and catalytic activity, however, depend on the type of metal dopant used. Thus, we investigated $CH_3OH$ interaction with isomorphous substitution of aluminum or phosphorus atoms by Mn, Zn, Mg or Si, Ti, Zr (MAPO-34) zeolites. (3) Three adsorption models of the initial structure of the interaction between MAPO-34 and the $CH_3OH$ molecule are considered, as shown in Figure 1.

In the present study, theoretical interactions of $CH_3OH$ with MAPO-34 (M = Mn, Zn, Mg, Si, Ti, Zr) zeolites were investigated to gain an understanding of the mechanism involved at the electronic molecular level. This understanding represents a basis for the rational design of improved catalysts.

**TABLE 1: Structural Parameters (Å) and Adsorption Energies (kcal/mol) for the Adsorption of $CH_3OH$ onto the Cluster MAPO-34 (M = Mn, Zn, Mg) at the B3LYP/LANL2DZ-6-31G** Level**

| | $O_m-H_z$ | $O_m-H_m$ | $O_z-H_z$ | $O_z-H_m$[a] | $H_m-H_z$ | C−O | $E_{ads}$ |
|---|---|---|---|---|---|---|---|
| Mn | 1.080 | 1.028 | 1.371 | 1.524 | 1.626 | 1.462 | 33.59 |
| Zn | 1.073 | 1.019 | 1.398 | 1.567 | 1.604 | 1.468 | 20.81 |
| Mg | 1.047 | 1.031 | 1.446 | 1.557 | 1.582 | 1.465 | 29.83 |

[a] Distance of the methanol proton to the closest framework oxygen atom.

## 2. Computational Methods and Models

Bronsted acid sites are introduced in MAPO-34 when divalent $Mn^{2+}$, $Zn^{2+}$, and $Mg^{2+}$ ions replace $Al^{3+}$ or tetravalent $Si^{4+}$, $Ti^{4+}$, and $Zr^{4+}$ ions replace $P^{5+}$, with protonation of one of its four nearest−neighbor oxygen ions in the framework.

**2.1. Cluster Approach.** All computations were performed within Gaussian 03[47] using the B3LYP[48,49] density functional, which yields accurate results for the molecular structures and vibrational frequencies of zeolite.[50,51] The standard double-$\xi$ basis set, as reported by Hay and Wadt[52] and denoted as LANL2DZ, is used to describe the electron density of the valence electrons of Mn, Zn, Mg, Ti, Zr, whereas the electron density of Si, Al, O, C, and H atoms is described using the standard 6-31G** basis set. It should also be noted that all energy values reported include corrections for zero-point energy because of their partial optimizations. In this study, basis-set-superposition-error (BSSE) corrections were not made for three reasons: (1) BSSE is expected to be approximately the same

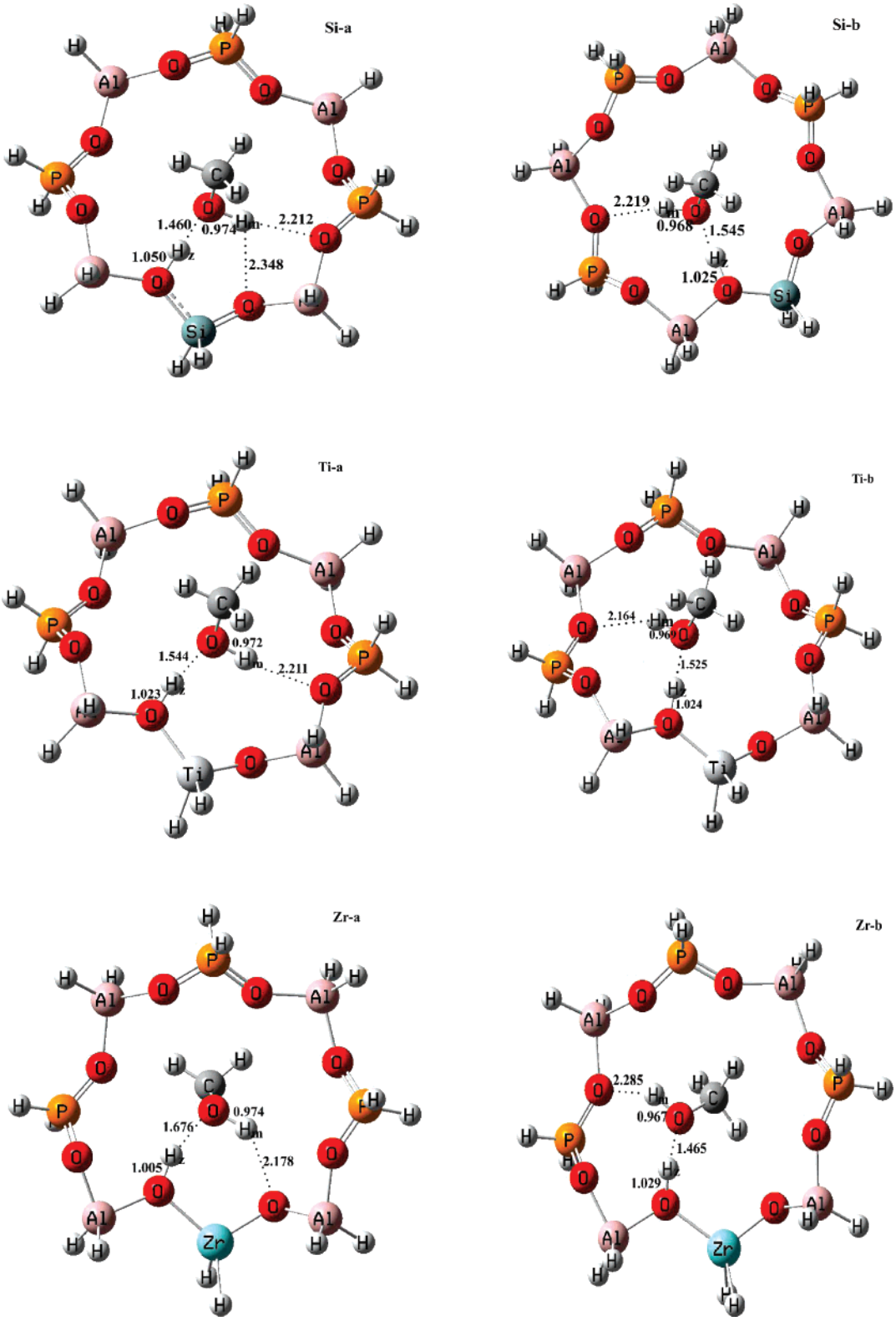


**Figure 3.** Equilibrium geometry found for $CH_3OH$ adsorbed on Si-, Ti-, and Zr-AlPO-34 with the cluster models. Selected bond distances are given in angstroms.

for each of the clusters examined;[53] (2) we are only interested in the adsorption complex in terms of the substituents nature; (3) we focused on change trends for the adsorption energy between methanol and the metal-modified zeolite.

An 8T ring was cut from AlPO-34, with dangling Al and Si bonds saturated by hydrogens atoms. To mimic the geometry constraints of the real zeolite structure in the calculations, we included terminating hydrogen atoms with fixed Cartesian coordinates at initial positions of 1.46 Å (Si−H) and 1.55 Å (Al−H) along the tetrahedral (T) bond. Geometry optimization calculations were carried out to obtain a local minimum for adsorption complexes.

**2.2. Periodical Approach.** Comparative calculations based on a generalized gradient approximation (GGA) in DFT with the periodic model were carried out using the DMol[3] program from Accelrys.[54] The Perder−Burke−Ernzerhof (PBE) exchange

and correlation functional,[55,56] and the double-numeric-polarized (DNP)[57−59] basis set was also used. The DNP, all-electron basis set comprises two numerical functions per valence orbital, supplemented with a polarization function. Each basis function was restricted to within a cutoff radius of $R_{cut} = 4.0$ Å, thereby allowing for efficient calculations without a significant loss of accuracy. The DMol[3] program uses numerical functions that are far more complete than the traditional Gaussian functions, and therefore we expect BSSE contribution to be small.[33,34]

## 3. Results and Discussion

The methanol system was chosen as a test case for the present DFT methods. To test the validity of our methods for handling hydrogen bonding, the energy for methanol dimmer formation was calculated using the two approaches. The values of 5.70 and 5.85 kcal/mol for the cluster and periodic calculations, respectively, compare well with the experimentally estimated range of 4.6−5.9 kcal/mol.[60]

Although it is known from spectroscopic evidence that methanol is initially adsorbed at Bronsted acid sites,[61] the mechanism is still a matter of much debate. The first point concerns whether both the physisorbed and chemisorbed methanol structures correspond to minima on the potential energy surface and, if so, which is more stable. Finite cluster calculations have shown that only the unprotonated form of methanol corresponds to a minimum for a 3T site model.[62] The methoxonium ionlike structure was identified as a transition state for proton transfer between two framework oxygen atoms.[23] Later, contradictory to the 3T cluster calculations, a methoxonium cation was found to correspond to a local minimum rather than a transition state for methanol adsorbed in 8T rings of chabazite[29,63] or gerieirte.[29] On the other hand, periodic calculations[63] revealed that the nature of the adsorbed methanol species can depend on the particular zeolite structure. Second, there are a large number of ways in which methanol can bind to the Bronsted acid site of a zeolite catalyst. In the present study, three starting geometries were considered: 6-M (six-membered ring, bridging across metal), 6-Al (P) (six-membered ring, bridging across Al or P), and side-on (side-on geometry, bridging across metal), as shown in Figure 1. The interaction between isomorphously substituted MAPO-34 (M = Mn, Zn, Mg, Si, Ti, Zr), and $CH_3OH$ was then investigated using cluster and periodic methods, which are discussed in the following.

**3.1. Cluster Approach.** Previous cluster-based studies[24,62] suggested the formation of a six-member ring arrangement for the methanol OH group and a zeolite O−Al−O(H) group. In the present study, three adsorption cases were considered for methanol adsorption on MAPO-34 (M = Mn, Zn, Mg, Si, Ti, Zr) (Figure 1).

In all three cases, when the structures were allowed to relax to the closest local energy minimum, the same geometry as for the chemisorbed form was observed for Mn, Zn, and Mg. It proved impossible to locate a minimum corresponding to simply methanol physisorption, and thus, we conclude that for this geometry the protonated form of adsorbed methanol is the most stable, without a barrier for proton transfer. The geometry of the stable complex is illustrated in Figure 2. Table 1 lists the adsorption energy values and structural parameters for $CH_3OH$ adsorbed onto the MAPO-34 (M = Mn, Zn, Mg) surfaces. The adsorption energy ($E_{ads}$) is calculated according to the formula

$$E_{ads} = E_{(cluster)} + E_{(CH_3OH)} - E_{(cluster + CH_3OH)}$$

**TABLE 2: Adsorption Modes, Structural Parameters (Å), and Adsorption Energies (kcal/mol) for the Adsorption of $CH_3OH$ onto the Cluster MAPO-34 (M = Si, Ti, Zr) at the B3LYP/LANL2DZ-6-31G** Level**

| | mode | $O_m-H_z$ | $O_m-H_m$ | $O_z-H_z$ | $O_z-H_m$[a] | $H_m-H_z$ | C−O | $E_{ads}$ |
|---|---|---|---|---|---|---|---|---|
| Si | a | 1.460 | 0.974 | 1.050 | 2.212 | 1.941 | 1.438 | 19.08 |
| | b | 1.545 | 0.968 | 1.025 | 2.219 | 2.129 | 1.442 | 17.05 |
| Ti | a | 1.544 | 0.972 | 1.023 | 2.211 | 2.085 | 1.435 | 15.78 |
| | b | 1.525 | 0.969 | 1.024 | 2.164 | 2.069 | 1.435 | 14.76 |
| Zr | a | 1.676 | 0.974 | 1.005 | 2.178 | 2.128 | 1.435 | 13.35 |
| | b | 1.465 | 0.967 | 1.029 | 2.285 | 2.048 | 1.441 | 13.27 |

[a] Distance of the methanol proton to the closest framework oxygen atom.

where $E_{(cluster)}$, $E_{(CH_3OH)}$, and $E_{(cluster + CH_3OH)}$ denote the energy calculated for a cluster without $CH_3OH$, the free $CH_3OH$, and a cluster with $CH_3OH$, respectively. The adsorption energy for $CH_3OH$ adsorbed onto a periodic model was calculated similarly.

From Figure 2, it is clearly evident that $CH_3OH$ is chemisorbed onto MAPO-34 (M = Mn, Zn, Mg), involving methanol bridging across the metal defect (see Figure 2) with the formation of a six-member ring arrangement. The methoxonium cation ($CH_3^-OH_2^+$) forms two very strong hydrogen bonds with the negatively charged zeolite. The $O_mH_z$ distance of 1.047−1.089 Å agrees with the values reported by Mihaleva et al.[31] (1.110 and 1.052 Å) and Haase et al.[64] (1.101 and 1.058 Å). The $O_mH_m$ distance (1.019−1.031 Å) is greater compared to its equilibrium OH distance in covalent bonds (0.96−0.97 Å).

However, the methoxonium ion is not a stable species during methanol adsorption on MAPO-34 (M = Si, Ti, Zr). Instead, two physisorbed structures were identified. The first shown in Figure 3 has a methanol bridging across the metal defect. The second is similar, except the methanol bridges across the aluminum defect. The former configurations are relatively more stable by 8.5, 5.3, and 0.3 kJ/mol, respectively. Values for the adsorption energy and the geometry of a methanol molecule interacting with the zeolite clusters are listed in Table 2. The equilibrium structures of the acidic sites and of the methanol adsorption complexes of all zeolites studied are remarkably similar. Methanol interacts with the zeolite framework through two hydrogen bonds to form an eight-member ring. One is through the bridging hydroxyl species of the zeolite cluster model, and the other weaker hydrogen bond is formed by an oxygen atom of the zeolite framework. The two structures for $CH_3OH$ adsorbed on SiAPO-34 differ in terms of methanol coordination: in the latter, the methanol proton forms a single hydrogen bond with the ring, whereas in the former, a bifurcated hydrogen bond is formed. A slightly different configuration is observed for the Zr-a, which is a six-member ring. The oxygen atom of methanol ($O_m$) is in close interaction with the cluster acid proton ($H_z$): the $O_mH_z$ distance is between 1.46 and 1.68 Å. For Si, Ti, and Zr-AlPO-34, there was no evidence of methanol protonation.

The $H_m-H_z$ distances were between 1.58 Å (MgAPO-34) and 1.63 Å (MnAPO-34) (Table 1) for the methoxonium ion complexes and between 1.94 Å (SiAPO-34) and 2.13 Å (ZrAPO-34) for the neutral complex (Table 2). These results are in good agreement with the values of 1.81−1.92 Å and 1.57 Å calculated for the neutral complex and the ion-pair complex, respectively.[65,66] All calculations suggest that whether the methanol is protonated or not by the MAPO-34 (M = Mn, Zn, Mg, Si, Ti, Zr) zeolite has little effect on the methanol C−O bond, in agreement with previous calculations.[41,67,68]

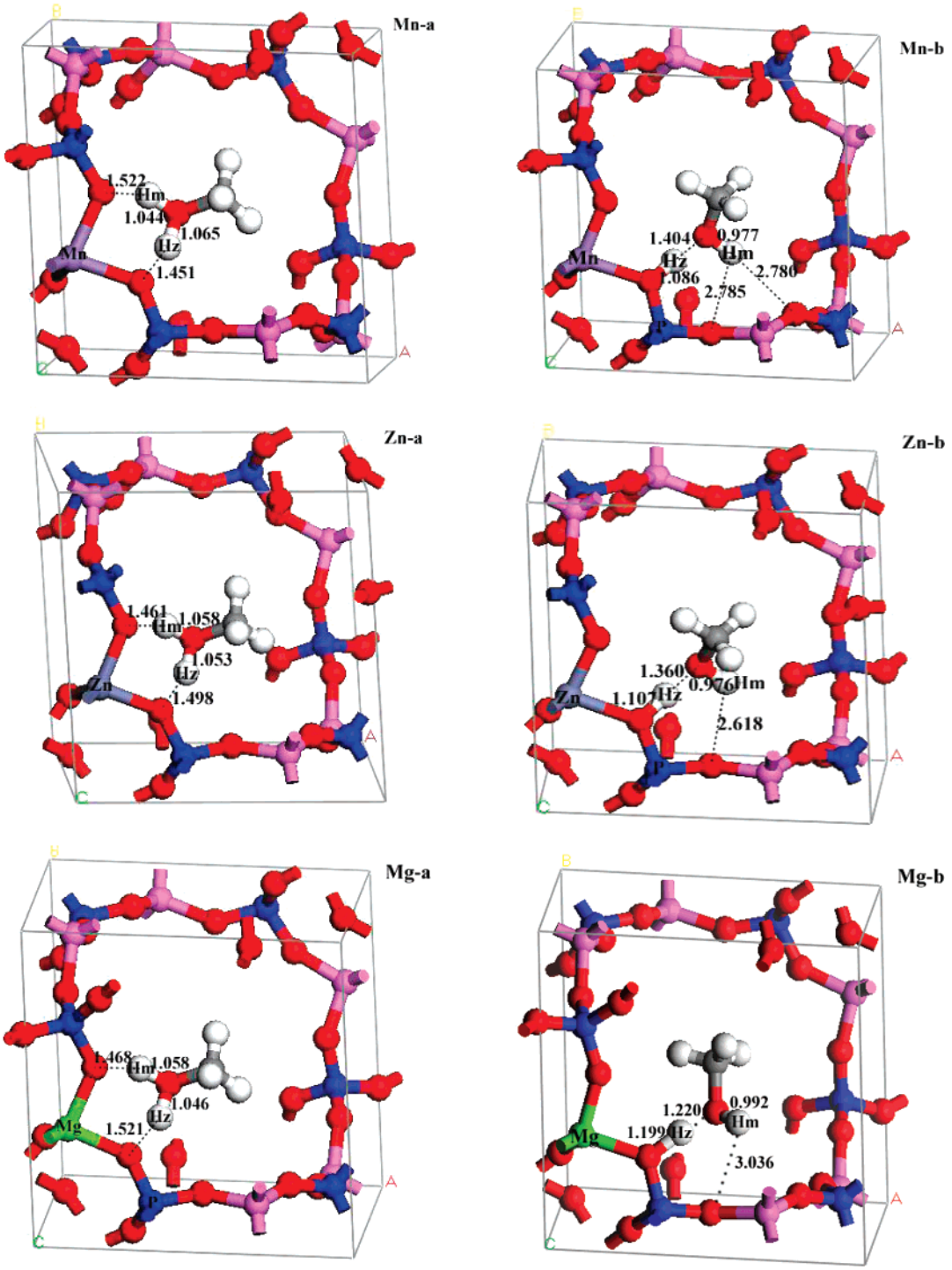


**Figure 4.** Equilibrium geometry found for $CH_3OH$ adsorbed on Mn-, Zn-, and Mg-AlPO-34 with the periodic models. Selected bond distances are given in angstroms.

To obtain a better insight into the influence of the zeolite lattice on adsorbed methanol and the adsorption complexes, periodical crystal calculations are necessary.

**3.2. Periodical Approach.** To compare the cluster calculations, methanol adsorbed on the three different modes is also considered using periodic calculations. In the case of periodic calculations, both physisorbed and chemisorbed adsorption structures for $CH_3OH$ adsorbed on MAPO-34 (M = Mn, Zn, Mg) were observed. For $CH_3OH$ adsorbed on the MAPO-34 (M = Mn, Zn, Mg), the chemisorbed adsorption structure has relatively higher adsorption energy of 20, 19, and 16 kJ/mol (Table 3), respectively, indicating that the preferred mode for $CH_3OH$ adsorption on MAPO-34 (M = Mn, Zn, Mg) is end-on chemisorption across the metal site. Similar to the cluster observations, relaxation of the $CH_3OH$ adsorption complex resulted in an equilibrium structure in which the acidic proton is transferred to the methanol yielding a methoxonium ion connected to the zeolite framework by two strong H bonds differing in length by approximately 0.021, 0.005, and 0.012 Å for Mn, Zn, and Mg, respectively (Figure 4; data for Si, Ti, and Zr, respectively, can be seen in Figure 5). $CH_3OH$ adsorbed on MnAPO-34 exhibited a physisorbed equilibrium structure with two intermolecular H bonds of nearly the same length (see Figure 4). Framework distortions of the eight-member ring allowed the methanol hydrogen atom to interact not with an oxygen atom belonging to the $AlO_4$ tetrahedron but with the

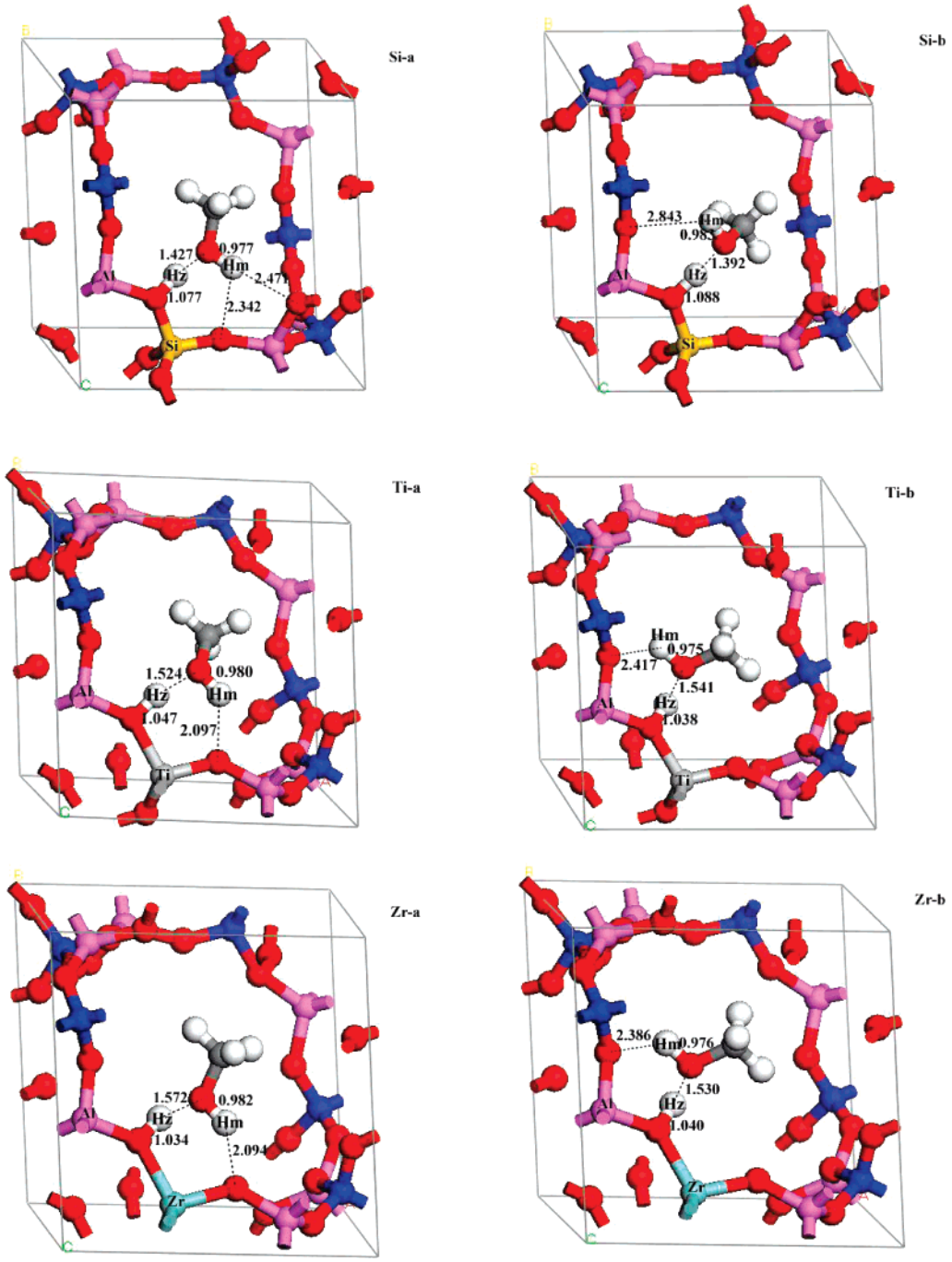


**Figure 5.** Equilibrium geometry found for $CH_3OH$ adsorbed on Si-, Ti-, and Zr-AlPO-34 with the periodic models. Selected bond distances are given in angstroms.

second nearest-neighbor oxygen in the eight-member ring as shown in Figure 4 (Mn-b). This is qualitatively the same as observations by Nusterer et al.[67] for sodalite calculations and by Haase[64] for chabazite calculations. With the change in model size from cluster to periodic, the adsorption energy changes by 1−6 kcal/mol for M = Zn, Mg. However, a significant change of 11 kcal/mol is observed for MnAPO-34.

Regarding the central question as to whether methanol is protonated or not, the same conclusion as for the cluster studies was observed for MAPO-34 (M = Si, Ti, Zr): the stable form of the adsorption complex is two physisorbed modes stabilized by one short and rather strong and one much weaker hydrogen bond. From Table 4, it is evident that the difference in adsorption energy between the two modes is small (0.1−12 kJ/mol). Interaction of the Bronsted acid proton with the O atom of $CH_3$-OH leads to slight elongation of the $O_zH_z$ bond distance but does not result in proton transfer. Hydrogen bonding between

**TABLE 3: Adsorption Modes, Structural Parameters (Å), and Adsorption Energies (kcal/mol) for the Adsorption of $CH_3OH$ onto the MAPO-34 (M = Mn, Zn, Mg) at the GGA/PBE Level**

| | mode | $O_m-H_z$ | $O_m-H_m$ | $O_z-H_z$ | $O_z-H_m$[a] | $H_m-H_z$ | C−O | $E_{ads}$ |
|---|---|---|---|---|---|---|---|---|
| Mn | a | 1.065 | 1.044 | 1.451 | 1.522 | 1.573 | 1.472 | 23.00 |
| | b | 1.404 | 0.977 | 1.086 | 2.785/2.78 | 1.977 | 1.458 | 18.23 |
| Zn | a | 1.053 | 1.058 | 1.498 | 1.461 | 1.568 | 1.471 | 21.67 |
| | b | 1.360 | 0.976 | 1.107 | 2.618 | 1.903 | 1.462 | 17.24 |
| Mg | a | 1.046 | 1.058 | 1.521 | 1.468 | 1.569 | 1.471 | 23.90 |
| | b | 1.220 | 0.992 | 1.199 | 3.036 | 1.836 | 1.461 | 20.10 |

[a] Distance of the methanol proton to the closest framework oxygen atom.

**TABLE 4: Adsorption Modes, Structural Parameters (Å), and Adsorption Energies (kcal/mol) for the Adsorption of $CH_3OH$ onto the Cluster MAPO-34 (M = Si, Ti, Zr) at the B3LYP/LANL2DZ-6-31G** Level**

| | mode | $O_m-H_z$ | $O_m-H_m$ | $O_z-H_z$ | $O_z-H_m$[a] | $H_m-H_z$ | C−O | $E_{ads}$ |
|---|---|---|---|---|---|---|---|---|
| Si | A | 1.427 | 0.977 | 1.077 | 2.34/2.47 | 1.894 | 1.451 | 16.00 |
| | B | 1.392 | 0.983 | 1.088 | 2.843 | 1.949 | 1.450 | 18.81 |
| Ti | A | 1.524 | 0.980 | 1.047 | 2.097 | 1.956 | 1.448 | 17.63 |
| | B | 1.541 | 0.975 | 1.038 | 2.417 | 1.983 | 1.453 | 17.76 |
| Zr | A | 1.572 | 0.982 | 1.034 | 2.094 | 2.034 | 1.449 | 17.42 |
| | B | 1.530 | 0.976 | 1.040 | 2.386 | 1.974 | 1.452 | 17.44 |

[a] Distance of the methanol proton to the closest framework oxygen atom.

the $O_z$ atom of the zeolite framework and the $H_m$ atoms of $CH_3$-OH is observed with a bond distance between 2.094 and 2.843 Å.

## 4. Conclusions

In the present work, the interaction of $CH_3OH$ with MAPO-34 (M = Mn, Zn, Mg, Si, Ti, Zr) was investigated using quantum chemical DFT calculations with the cluster and periodic models, which both yielded the same results for MAPO-34 (M = Si, Ti, Zr): the stable form of the adsorption complexes is two physisorbed methanol molecules stabilized by one short and rather strong and one much weaker hydrogen bond. In contrast, we found that a proton transfer without a barrier takes place in MAPO-34 (M = Mn, Zn, Mg) and that a chemisorbed methoxonium ion is the more stable structure of adsorbed methanol.

**Acknowledgment.** This work was supported by NSFC (20573110). K.L.H. is a member of Virtual Laboratory for Computational Chemistry, CNIC, CAS.

## References and Notes

(1) Meissel, S. L.; McCullogh, J. P.; Lechthaler, C. H.; Weisz, P. B. *Chem. Technol.* **1976**, *6*, 86.
(2) Stocker, M. *Microporous Mesoporous Mater.* **1999**, *29*, 3.
(3) Keil, F. J. *Microporous Mesoporous Mater.* **1999**, *29*, 49.
(4) Vora, B. V.; Marker, T. L.; Barger, P. T.; Fullerton, H. E.; Nilson, H. P.; Kvisile, S.; Fuglerud, T. *Stud. Surf. Sci. Catal.* **1997**, *107*, 87.
(5) Qi, G. Z.; Xie, Z. K.; Yang, W. M.; Zhong, S. Q.; Liu, H. X.; Zhang, C. F.; Chen, Q. L. *Fuel Process. Technol.* **2007**, *88*, 437.
(6) Weisz, P. B. *Pure Appl. Chem.* **1980**, *52*, 2091.
(7) Weisz, P. B.; Haag, W. O.; Lago, R. M. *Nature* **1984**, *309*, 589.
(8) Kang, M. *J. Mol. Catal. A* **2000**, *160*, 437.
(9) Kang, M. *J. Mol. Catal. A* **1999**, *150*, 205.
(10) Kang, M.; Lee, C. T. *J. Mol. Catal. A* **1999**, *150*, 213.
(11) Inui, T.; Kang, M. *App. Catal. A* **1997**, *164*, 211.
(12) Franklin, I. L.; Beale, A. M.; Sankar, Catal, G. *Today* **2003**, *81*, 623.
(13) Rajic, N.; Stojakovic, D.; Hocevar, S.; Kaucic, V. *Zeolite* **1993**, *13*, 384.
(14) Wei, Y. X.; He, Y. L.; Zhang, D. Z.; Xu, L. *Microporous Mesoporous Mater.* **2006**, *90*, 188.
(15) Yuan, S. P.; Wang, J. G.; Li, Y. W.; Peng, S. Y. *J. Mol. Catal. A* **2002**, *178*, 267.
(16) Yuan, S. P.; Wang, J. G.; Li, Y. W.; Jiao, H. J. *J. Phys. Chem. A* **2002**, *106*, 8167.
(17) Saadoune, I.; Cora, F.; Catlow, C. R. A. *J. Phys. Chem. B* **2003**, *107*, 3003.
(18) Limtrakul, J.; Khongpracha, P.; Jungsuttiwong, S.; Truong, T. N. *J. Mol. Catal. A* **2000**, *153*, 155.
(19) Brand, H. V.; Redondo, A.; Hay, P. J. *J. Phys. Chem. A* **1997**, *101*, 7691.
(20) Jobic, H.; Tuel, A.; Krossner, M.; Sauer, J. *J. Phys. Chem.* **1996**, *100*, 19545.
(21) Chu, C. T. W.; Chang, C. D. *J. Phys. Chem.* **1985**, *89*, 1569.
(22) Inui, T.; Matsuba, K. *Stud. Surf. Sci. Catal.* **1994**, *90*, 355.
(23) Blaszkowski, S. R.; Santen, R. A. *J. Phys. Chem.* **1995**, *99*, 11728.
(24) Blaszkowski, S. R.; Santen, R. A. *J. Am. Chem. Soc.* **1997**, *119*, 5020.
(25) Blaszkowski, S. R.; Santen, R. A. *J. Phys. Chem. B* **1997**, *101*, 2292.
(26) Blaszkowski, S. R.; Santen, R. A. *Top. Catal.* **1997**, *4*, 145.
(27) Haase, F.; Sauer, J. *J. Am. Chem. Soc.* **1995**, *117*, 3780.
(28) Gale, J. D.; Shah, R.; Payne, M. C.; Stich, I.; Terakura, K. *Catal. Today* **1999**, *50*, 525.
(29) Stich, I.; Gale, J. D.; Terakura, K.; Payne, M. C. *J. Am. Chem. Soc.* **1999**, *121*, 3292.
(30) Haase, F.; Sauer, J. *Microporous Mesoporous Mater.* **2000**, *35*, 379.
(31) Mihaleva, V. V.; Santen, R. A.; Jansen, A. P. J. *J. Phys. Chem. B* **2001**, *105*, 6874.
(32) Mihaleva, V. V.; Santen, R. A.; Jansen, A. P. J. *J. Chem. Phys.* **2003**, *119*, 13053.
(33) Govind, N.; Andzelm, J.; Reindel, K.; Fitzgerald, G. *Int. J. Mol. Sci.* **2002**, *3*, 423.
(34) Govind, N.; Fitzgerald, G.; King-Smith, D. *Int. J. Quantum Chem.* **2003**, *91*, 467.
(35) Kogelbauer, A.; Grundling, C.; Lercher, J. A. *J. Phys. Chem.* **1996**, *100*, 1852.
(36) Forester, T. R.; Howe, R. F. *J. Am. Chem. Soc.* **1987**, *109*, 5076.
(37) Kubelkova, L.; Novakova, J.; Nedomova, K. *J. Catal.* **1990**, *124*, 441.
(38) Tsiao, C. J.; Corbin, D. R.; Dybowski, C. *J. Am. Chem. Soc.* **1990**, *112*, 7140.
(39) Bosacek, V. *J. Phys. Chem.* **1993**, *97*, 10732.
(40) Haase, F.; Sauer, J. *J. Phys. Chem.* **1994**, *98*, 3083.
(41) Gale, J. D. *Top. Catal.* **1996**, *3*, 169.
(42) Van Santen, R. A. *J. Mol. Catal. A* **1997**, *115*, 405.
(43) Vos, A. M.; Rozanska, X.; Schoonheydt, R. A.; van Santen, R. A.; Hutschka, F.; Hafner, J. *J. Am. Chem. Soc.* **2001**, *123*, 2799.
(44) Zygmunt, S. A.; Curtiss, L. A.; Zapol, P.; Iton, L. E. *J. Phys. Chem. B* **2000**, *104*, 1944.
(45) Frash, M. V.; Van, Santen, R. A. *Top. Catal.* **1999**, *9*, 191.
(46) Ciobica, I. M.; Frechard, F.; van Santen, R. A.; Kleyn, A. W.; Hafner, J. *Chem. Phys. Lett.* **1999**, *311*, 185.
(47) Frisch, M. J.; Trucks, G. W.; Schlegel, H. B.; Scuseria, G. E.; Robb, M. A.; Cheeseman, J. R.; Zakrzewski, V. G.; Montgomery, J. A.; Stratmann, R. E.; Burant, J. C.; Dapprich, S.; Millam, J. M.; Daniels, A. D.; Kudin, K. N.; Strain, M. C.; Farkas, O.; Tomasi, J.; Barone, V.; Cossi, M.; Cammi, R.; Mennucci, B.; Pomelli, C.; Adamo, C.; Clifford, S.; Ochterski, J.; Petersson, G. A.; Ayala, P. Y.; Cui, Q.; Morokuma, K.; Rega, N.; Salwador, P.; Dannenberg, J. J.; Malick, D. K.; Rabuck, A. D.; Raghavachari, K.; Foresman, J. B.; Cioslowski, J.; Ortiz, J. V.; Baboul, A. G.; Stefanom, B. B.; Liu, G.; Liashenko, A.; Piskorz, P.; Komaromi, I.; Gomperts, R.; Martin, R. L.; Fox, D. J.; Keith, T.; Al.-Laham, M. A.; Peng, C. Y.; Nanayakkara, A.; Challacombe, M.; Gill, P. M. W.; Johnson, B.; Chen, W.; Wong, C. M. W.; Anders, J. L.; Gonzalez, C.; Head-Gordon, M.; Replogle, E. S.; Pople, J. A. *Gaussian 03*, revision A.11.4; Gaussian Inc, Pittsburgh, PA, 2003.
(48) Becke, A. D. *J. Chem. Phys.* **1993**, *98*, 5648.
(49) Lee, C.; Yang, W. T.; Parr, R. G. *Phys. Rev. B* **1988**, *37*, 785.
(50) Limtrakul, J.; Onthong, U. *J. Mol. Struct.* **1997**, *435*, 181.
(51) Limtrakul, J.; Treesukol, P.; Ebner, C.; Sansone, R.; Probst, M. *Chem. Phys.* **1997**, *215*, 77.
(52) Hay, P. J.; Wadt, W. R. *J. Chem. Phys.* **1985**, *82*, 299.
(53) Gonzales, N. O.; Chakraborty, A. K.; Bell, A. T. *Catal. Lett.* **1998**, *50*, 135.
(54) Dmol$^3$ from Accelrys: http://www.accelrys.com.
(55) Hohenberg, P.; Kohn, W. *Phys. Rev.* **1964**, *136*, B864.
(56) Perdew, J. P.; Burke, K.; Ernzerhof, M. *Phys. Rev. Lett.* **1996**, *77*, 3865.
(57) Delley, B. *J. Chem. Phys.* **1990**, *92*, 508.
(58) Delley, B. *J. Chem. Phys.* **1996**, *100*, 6107.
(59) Delley, B. *J. Chem. Phys.* **2000**, *113*, 7756.
(60) Szalewicz, K.; Jeziorski, B. *Molecular Interctions*; Scheiner, S., Ed.; John Wiley & Sons: New York, 1997; p 3.
(61) Mirth, G.; Lercher, J. A.; Anderson, W.; Klinowski, J. *J. Chem. Soc., Faraday Trans.* **1990**, *86*, 3039.
(62) Gale, J. D.; Catlow, C. R. A.; Carruthers, J. *R. Chem. Phys. Lett.* **1993**, *216*, 155.
(63) Shah, R.; Gale, J. D.; Payne, M. C. *J. Phys. Chem.* **1996**, *100*, 11688.
(64) Haase, F.; Sauer, J.; Hutter, J. *Chem. Phys. Lett.* **1997**, *266*, 397.
(65) Kubellkova, L.; Kotrla, J.; Florian, J.; Bolom, J.; Fraissard, J.; Heeribout, L.; Doremieux-Morin, C. *Proceedings of the 11th International Congress on Catalysis*; Baltimore, 1996.
(66) Stich, I.; Gale, J. D.; Terakura, K.; Payne, M. C. *Chem. Phys. Lett.* **1998**, *283*, 402.
(67) Nusterer, E.; Blochl, P. E.; Schwarz, K. *Angew. Chem., Int. Ed.* **1996**, *35*, 175.
(68) Shah, R.; Payne, M. C.; Lee, M. H.; Gale, J. D. *Science* **1996**, *271*, 1395.